

Hydrothermal Synthesis and Characterization of the Thorium Phosphate Hydrogenphosphate, Thorium Hydroxide Phosphate, and Dithorium Oxide Phosphate

V. Brandel,¹ N. Dacheux, and M. Genet

Institut de Physique Nucléaire, Groupe de Radiochimie, Université de Paris XI, Bât. 100, 91406 Orsay, France

and

R. Podor

Faculté des Sciences, Laboratoire de Chimie du Solide Minéral, Université H. Poincaré, Nancy I, B.P. 239, 54506 Vandœuvre-lès-Nancy Cedex, France

Received November 15, 2000; in revised form March 7, 2001; accepted March 15, 2001; published online May 11, 2001

Because of its low solubility in water and high thermal stability, thorium phosphate diphosphate (TPD), $\text{Th}_4(\text{PO}_4)_4\text{P}_2\text{O}_7$, seems to be a very good matrix for radionuclide immobilization. During the leaching studies of this compound the formation of a new phase, different from the TPD was observed. In order to identify this phase, two other thorium phosphates: thorium phosphate–hydrogenphosphate (TPHP), $\text{Th}_2(\text{PO}_4)_2\text{HPO}_4 \cdot \text{H}_2\text{O}$, and thorium hydroxide phosphate (THOP), $\text{Th}(\text{OH})\text{PO}_4$, were synthesized in hydrothermal conditions then characterized. It appeared that the neoformed phase was identical to the TPHP. © 2001 Academic Press

Key Words: hydrothermal synthesis; thorium phosphate–hydrogenphosphate; thorium hydroxide phosphate; dithorium oxide phosphate.

INTRODUCTION

Thorium phosphate–diphosphate (TPD), $\text{Th}_4(\text{PO}_4)_4\text{P}_2\text{O}_7$, was proposed as a promising matrix for long-term radionuclide immobilization (1–4), especially for tetravalent actinides like uranium, neptunium, and plutonium incorporated in the TPD structure (5) as solid solutions (6, 7). Before using a matrix for the radioactive waste storage, it is necessary to investigate its resistance to water corrosion. During the leaching tests of the TPD it was noticed that thorium Th^{4+} and phosphate PO_4^{3-} ions are very slowly released into the solution (8, 9). Indeed, these ions are dissociated in water to give different species depending on the acidity, e.g., ThOH^{3+} and HPO_4^{2-} . The diphosphate ion

$\text{P}_2\text{O}_7^{4-}$ is also transformed into the HPO_4^{2-} ion, even at room temperature. That is the main reason why a chemical equilibrium solid-solution between the TPD and its constituent ions cannot be considered from a thermodynamic point of view. Moreover, species in the solution obtained from the dissolved TPD can react to form a new solid in which the chemical composition differs from that of the TPD (10). Because of the very slow dissolution kinetics of the TPD in water it was impossible to study this phenomenon in a short time. In order to accelerate this process it was heated at 90°C with 5 M nitric acid in closed containers (8, 9). In fact, the initial TPD was transformed into another solid in which the X-ray diffraction (XRD) diagram is different from that of TPD. No XRD data, corresponding to this compound, were found neither in the JPDS files nor in the literature.

The aim of this work was to synthesize, identify, then characterize two thorium phosphates supposed to be identical to the neoformed phase, in acid solutions by hydrothermal conditions.

In the dissolution process of TPD, the mole ratio $(\text{PO}_4)/\text{Th}$ in the new solid may be the same as in the initial matrix, i.e., 3/2, or lower, equal for example to 1. According to these stoichiometries, thorium phosphate–hydrogenphosphate or thorium hydroxide phosphate could be the reaction products. Thorium phosphate–hydrogenphosphate (TPHP), $\text{Th}_2(\text{PO}_4)_2\text{HPO}_4 \cdot n\text{H}_2\text{O}$ ($n = 3-7$) as amorphous phase was already synthesized by precipitation from thorium nitrate or thorium chloride concentrated solution and phosphoric acid (11). Notice that thorium phosphate–hydrogenphosphate is a precursor of the TPD. Thorium hydroxide phosphate (THOP) is unknown but is probably analogous with the uranium hydroxide phosphate

¹To whom correspondence should be addressed. E-mail: brandel@ipno.in2p3.fr.

(12). Uranium-like thorium is an actinide element, therefore the properties of uranium (IV) compounds present similarities with the thorium compounds. Because their XRD diagrams are unknown, it was very useful to compare them with the existing uranium phosphates.

Several physico-chemical methods were used for characterization and identification of the obtained compounds. Electron probe microanalysis (EPMA) allowed us to define the quantitative amounts of thorium and phosphorus and the purity of the products. The recorded infrared (IR) spectra were complementary in order to give evidence of chemical bonds and therefore of some groups of atoms (also, to compare to other compounds with similar function groups). Finally, thermal analyses showed the transformation of the synthesized products during the heating treatment.

EXPERIMENTAL

Chemicals and Apparatus

Thorium chloride solution was from Rhône-Poulenc (France). Other chemical reagents were supplied by Merck and Aldrich-Fluka.

For hydrothermal syntheses, Parr Instrument Company autoclaves supported with polytetrafluoroethylene (PTFE) containers (maximum volume 23 ml) were used. In order to increase the kinetics of the synthesis reaction, samples were heated to 100, 150, or 240°C. The vapor pressure in these containers (depending on the temperature) may raise up to 300 bars.

The X-ray powder diffraction (XRD) data were collected with a Philips PW 1050/70 diffractometer using the monochromatic $\text{CuK}\alpha$ radiation and a nickel filter. Patterns were recorded from 5 to 60° or 10 to 60° (2θ) with a step of 0.01° using silicon powder as internal reference. The refinement of the cell parameters was obtained using the U-Fit program (13).

The infrared (IR) spectra were recorded from 4000 to 400 cm^{-1} with an Hitachi I-2001 spectrophotometer. Samples of 1–1.5 wt% of the solids were prepared in KBr pellets.

The samples' heat treatment (with a rate of 5°C/min) was performed in alumina crucibles in a Pyrox MDB15 furnace.

Electron probe microanalyses (EPMA) were carried out by means of a CAMECA SX 50 apparatus working usually with a 15 kV voltage and a 10 nA current beam. ThO_2 ($M\alpha$ ray of thorium) and $\text{Ca}_5(\text{PO}_4)_3\text{OH}$ ($K\alpha$ ray of phosphorous) were used as calibration references.

Thermal gravimetric analysis (TGA) and differential thermal analysis (DTA) results were obtained with a SETARAM TG-DTA92 apparatus. Samples were heated in air, in Pt-Rh crucibles up to 1200°C with a heating rate 5°C/min.

Micrographs were carried out with a PHILIPS XL30 scanning electron microscope (SEM).

Samples Preparation

Powdered samples of thorium phosphates were prepared from a mixture of 1 M thorium nitrate solutions and 1–5 M phosphoric acid. The exact concentrations of the solutions were determined by conventional analytical methods.

Thorium phosphates. Three different procedures were applied for syntheses of thorium phosphate with the mole ratio

$$\frac{\text{H}_3\text{PO}_4}{\text{Th}} = \frac{3}{2}$$

1. Thorium nitrate solution was mixed with phosphoric acid in PTFE containers, diluted to a volume of 5 ml, then put in the autoclave and heated in an oven for two months;
2. The same kind of mixture was first dried on a sand bath at 150°C until a dry residue was obtained. Afterward, 10 ml of deionized water was added to the ground residue. The suspension was decanted in a PTFE container then heated in an autoclave for two months at 150°C;
3. Amorphous thorium phosphate-hydrogenphosphate was suspended in deionized water or in 0.1 M HNO_3 and then heated in a PTFE container for two months for crystal growth at 150°C.

Thorium phosphate with the mole ratio

$$\frac{\text{H}_3\text{PO}_4}{\text{Th}} = \frac{1}{1}$$

was synthesized by mixing thorium nitrate solution with phosphoric acid using the same conditions as described above.

Uranium phosphates. Uranium hydroxide phosphate (UHOP), $\text{U}(\text{OH})\text{PO}_4 \cdot 2\text{H}_2\text{O}$, was also prepared using the hydrolyzed uranium bromide phosphate (12).

Uranium hydrogenphosphate (UHP), $\text{U}(\text{HPO}_4)_2 \cdot 4\text{H}_2\text{O}$, was synthesized using the hydrothermal method (for 1 month) from uranium dioxide UO_2 and phosphoric acid.

After synthesis, all the samples were filtered, washed with deionized water, then dried at 100°C.

RESULTS AND DISCUSSION

Thorium Phosphate-Hydrogenphosphate

The electron probe microanalysis EPMA of the thorium phosphate-hydrogenphosphate, obtained from the direct synthesis, led to the mole ratio

$$\frac{\text{P}}{\text{Th}} = \frac{3}{2}$$

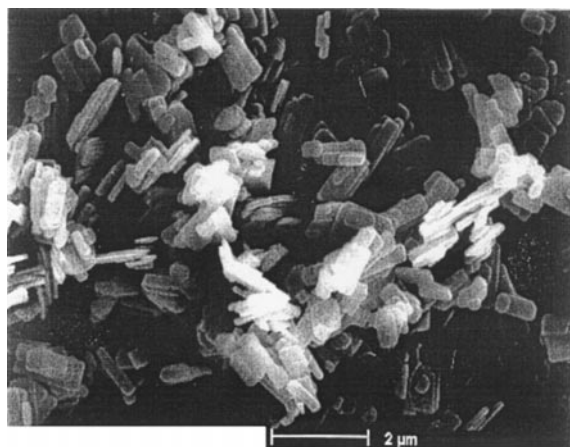


FIG. 1. SEM micrograph of the thorium phosphate–hydrogenphosphate.

As it can be seen from the SEM micrograph presented in Fig. 1, the dimension of the crystals does not exceed 1 μm . The product was single phase.

The recorded XRD diagram of this compound is shown in Fig. 2 and the corresponding data are given in Table 1. The same kind of diagram was obtained for all samples, independent of the method of synthesis.

The IR spectrum of the synthesized product is presented in Fig. 3a, whereas the assigned bands are gathered in

TABLE 1
X-Ray Powder Diffraction Data of the Thorium Phosphate–Hydrogenphosphate (TPHP)

$2\theta_{\text{exp}}(^{\circ})$	$d_{\text{exp}}(\text{\AA})$	I/I_0	$2\theta_{\text{exp}}(^{\circ})$	$d_{\text{exp}}(\text{\AA})$	I/I_0
8.12	10.89	12	34.73	2.58	13
13.65	6.49	21	35.65	2.52	9
16.41	5.40	100	40.90	2.21	12
17.94	4.94	8	42.10	2.15	46
18.59	4.77	12	44.57	2.03	10
21.88	4.06	33	45.58	1.99	7
24.82	3.59	48	47.18	1.93	13
25.13	3.54	24	48.34	1.88	6
26.44	3.37	11	48.90	1.86	4
27.50	3.24	9	49.81	1.83	26
27.82	3.21	9	50.13	1.83	26
29.32	3.05	29	50.65	1.82	26
30.23	2.96	26	51.81	1.76	7
31.20	2.87	5	52.70	1.74	10
31.87	2.81	6	53.75	1.71	10
32.18	2.78	6	54.82	1.67	6
33.42	2.68	13	57.87	1.59	6
34.28	2.62	25			

Table 2. The broad band observed from 3650 to about 2700 cm^{-1} includes the O–H stretching modes of the water molecule and of the (P)–O–H group (14, 15), while the band observed at 1638 cm^{-1} is characteristic of the H_2O bending

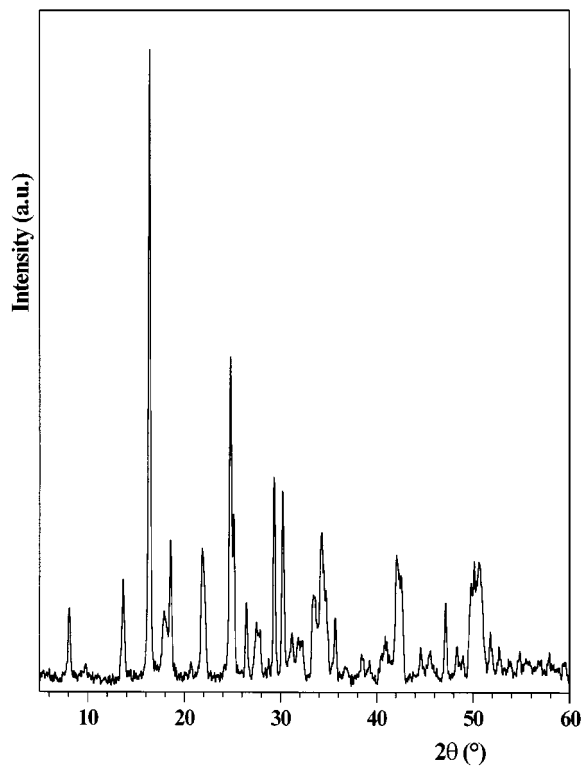


FIG. 2. XRD diagram of the thorium phosphate–hydrogenphosphate.

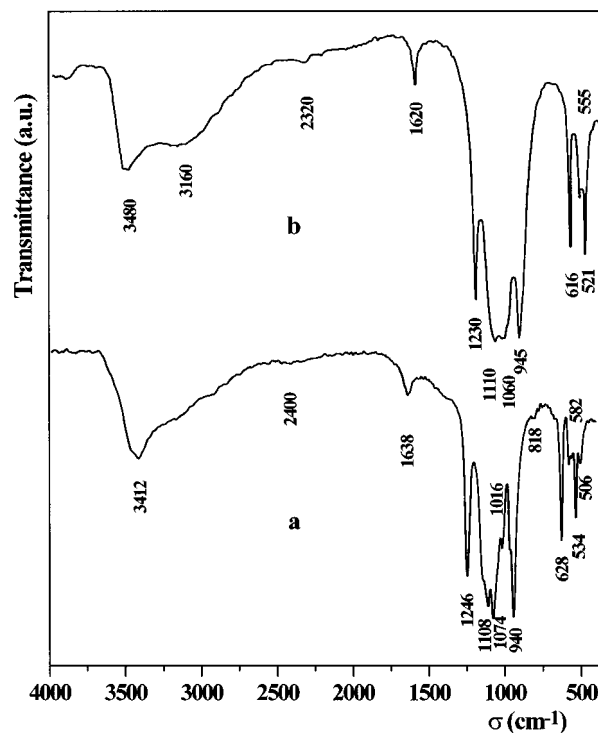


FIG. 3. IR spectra of the (a) thorium phosphate–hydrogenphosphate and the (b) uranium hydrogenphosphate.

TABLE 2

Assignment of the Vibrational Frequencies of the Thorium Phosphate–Hydrogenphosphate (TPHP) and the Uranium Hydrogenphosphate (UHP)

TPHP	UHP	Assignment
$\sigma(\text{cm}^{-1})$	$\sigma(\text{cm}^{-1})$	
3650–2700	3650–3700	stretching O–H and (P)–O–H
\approx 2400 shoulder	\approx 2320 shoulder	stretching (P)–O–H
1638	1620	bending H_2O
\approx 1400 shoulder	\approx 1400 shoulder	bending (P)–O–H
1246	1230	stretching in the plane P–O–H
1108–940	1110–945	ν P–O
628–506	616–521	δ P–O

mode. The very weak shoulder at 2400 cm^{-1} may be also assigned to the (P)–O–H stretching vibrations (16). The bands observed from 1100 to 500 cm^{-1} correspond to the symmetric and asymmetric vibrations of the P–O bond, including bending modes of O–P–O of the PO_4 tetrahedron (16–18).

The band located at 1246 cm^{-1} may be assigned to the stretching mode in the plane of the P–O–H bonds in the HPO_4 group as observed at 1256 cm^{-1} for the disodium hydrogenphosphate $\text{Na}_2\text{HPO}_4 \cdot 2\text{H}_2\text{O}$ (14). It seems that bands located between 1200 and 1400 cm^{-1} are characteristic of the HPO_4 group in crystallized hydrogenphosphates. For example, in the IR spectra of BaHPO_4 and $\beta\text{-SrHPO}_4$ frequencies near 1260 cm^{-1} are observed, for $\alpha\text{-SrHPO}_4$ and CoHPO_4 they are observed at 1300 cm^{-1} , whereas for $(\text{NH}_4)_2\text{HPO}_4$ the band is located at 1250 cm^{-1} (19).

In the IR spectrum of the amorphous TPHP, broad bands extend from 1400 to 800 cm^{-1} , approximately (11), and the HPO_4 group cannot be defined. The IR spectrum of the crystallized TPHP should be compared to that of the crystallized thorium hydrogenphosphate (THP) $\text{Th}(\text{HPO}_4)_2$. Unfortunately, only the amorphous or fibrous forms of this compound is described in the literature (20–22); no data (XRD or IR) for a crystallized THP were found. Thus, the IR spectrum of the crystallized TPHP was compared to that of uranium hydrogenphosphate $\text{U}(\text{HPO}_4)_2 \cdot 4\text{H}_2\text{O}$ for which XRD data were published by Dunn (23). The spectra of both compounds are similar, as can be seen in Fig. 3. The frequencies observed at 1246 and 1230 cm^{-1} for TPHP and UHP, respectively, confirm the existence of the HPO_4 group. These bands as well as those

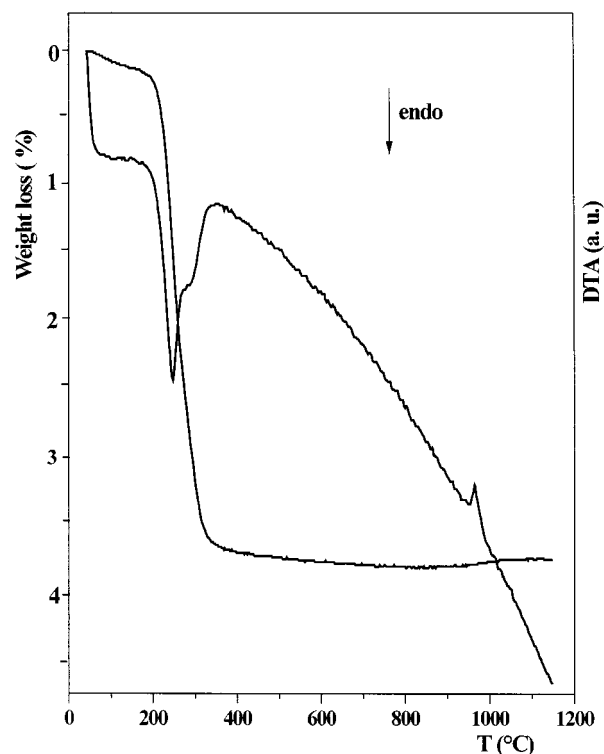


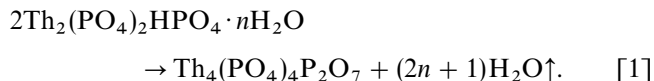
FIG. 4. TGA and DTA curves of the thorium phosphate–hydrogenphosphate.

corresponding to the stretching mode of O–H, (P)–O–H, or H–O–H bending mode, disappear when TPHP or UHP are heated at high temperature (950 – 1000°C). At these temperatures the TPHP is transformed into the TPD while UHP forms the uranium diphosphate $\alpha\text{-UP}_2\text{O}_7$. IR spectra of TPD and $\alpha\text{-UP}_2\text{O}_7$ were published in our previous work (11, 24, 25).

For many oxides, hydroxides, phosphates, and other metal-oxoanion salts, the metal–oxygen (M–O) stretching modes are usually observed, below 400 cm^{-1} (17), and can be also observed for some compounds in the 700 – 800 cm^{-1} range (15), e.g., narrow bands at about 725 cm^{-1} in the spectra of ThO_2 and UO_2 (19). In the TPHP and UHP spectra, the Th–O and U–O modes cannot be seen because of the overlap with the P–O or O–H bands. Only a very weak peak which appears at 808 cm^{-1} for TPHP (Fig. 3a) could be assigned to the Th–O bond.

During thermal treatment of the crystallized TPHP, a total weight loss occurs at about 450°C (TGA curve) while an endothermic band extending from 200 to 350°C appears simultaneously on the DTA curve (Fig. 4). Furthermore, a weak exothermic peak appears on the DTA curve at 950°C . This peak corresponds to the crystallization temperature of the thorium phosphate–diphosphate. The same type of DTA curve was obtained by heating the amorphous thorium phosphate–hydrogenphosphate (11). Taking into

account all the results presented, the decomposition reaction of the TPHP can be written as

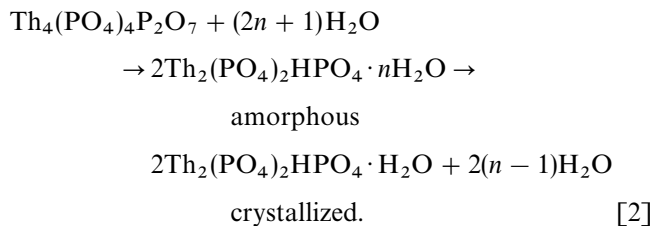


The average weight loss at 450°C, calculated from the TGA results, is equal to 3.6%, which corresponds to the loss of 3 moles of water for 2 moles of TPHP. From Eq. [1] the n value is thus equal to 1.03, which leads to the formula: $\text{Th}_2(\text{PO}_4)_2\text{HPO}_4 \cdot \text{H}_2\text{O}$, i.e., thorium phosphate–hydrogenphosphate monohydrate.

A crystallized compound with a mole ratio similar to TPHP was already reported in a previous publication (26). This solid, of which the formula was proposed as $\text{HTh}_2(\text{PO}_4)_3$, was synthesized hydrothermally from powdered ThO_2 and an excess of concentrated phosphoric acid; its XRD diagram differs from that of TPHP.

The TPD dissolution was already extensively studied. In order to accelerate the kinetics of the process, leaching tests were performed in 5 M nitric acid (8, 9). Under these conditions, the precipitation of a new phase was observed after 200 days at 90°C; it is first amorphous then slowly transforms to the crystallized form. The crystallized part of the product was analyzed and identified as $\text{Th}_2(\text{PO}_4)_2\text{HPO}_4 \cdot \text{H}_2\text{O}$. The other part corresponds to the amorphous $\text{Th}_2(\text{PO}_4)_2\text{HPO}_4 \cdot n\text{H}_2\text{O}$. The calculated solubility product value $K_{s,0}^*$ of the TPHP is estimated to be $10^{-66.6 \pm 1.2}$ (8, 9, 27).

The dissolution process of the TPD may be presented as follows: thorium phosphate diphosphate is dissolved in a reaction with the hydrogen ion forming more or less hydrolyzed species, depending on the pH of the medium. The intermediate reactions involve the formation of an amorphous layer (thickness about 20 nm, mole ratio $\text{PO}_4/\text{Th} = \frac{3}{2}$) which seems to control the dissolution of the TPD (8, 9). The global process can be presented as



Thorium Hydroxide Phosphate and Dithorium Oxide Phosphate

The mole ratio P/Th = 1/1 of the synthesized product (as a single phase) was confirmed by means of electron probe microanalysis (EPMA), the XRD data are shown in Table 3. Like the TPHP, this is also a well-crystallized compound

TABLE 3
X-Ray Powder Diffraction Data of the Thorium Hydroxide Phosphate (THOP)

$2\theta_{\text{exp}} (^{\circ})$	$d_{\text{exp}} (\text{\AA})$	I/I_0	$2\theta_{\text{exp}} (^{\circ})$	$d_{\text{exp}} (\text{\AA})$	I/I_0
13.98	6.33	28	42.86	2.11	7
17.04	5.20	2	43.22	2.09	7
19.01	4.67	100	44.59	2.03	31
20.29	4.38	57	46.19	1.97	5
21.00	4.23	26	47.26	1.92	4
23.75	3.75	33	47.63	1.91	6
24.78	3.59	11	48.43	1.88	4
26.39	3.38	4	48.68	1.87	5
28.37	3.15	6	48.84	1.86	5
28.64	3.12	30	49.00	1.86	5
31.46	2.84	5	50.49	1.81	3
32.33	2.78	43	51.01	1.79	3
32.58	2.75	29	51.33	1.78	31
34.61	2.59	24	51.77	1.77	14
38.33	2.35	5	53.73	1.71	11
39.43	2.29	20	54.52	1.68	4
40.81	2.21	7	59.75	1.55	3
41.60	2.17	5			

with crystal dimensions from about 2 to 8 μm (Fig. 5); its XRD diagram (Fig. 6a) presents some similarities with the uranium (IV) hydroxide phosphate (Fig. 6b) $\text{U}(\text{OH})\text{PO}_4 \cdot 2\text{H}_2\text{O}$ (JCPDS-ICDD File 38-397). However, the line intensities differ for both compounds and the UHOP lines are slightly shifted compared to those of THOP. The powder diffraction data of the THOP are presented in Table 3.

Close similarities were observed in the IR spectra of both compounds (Table 4 and Fig. 7). The strong narrow bands at around 3600 cm^{-1} were assigned to the O–H stretching

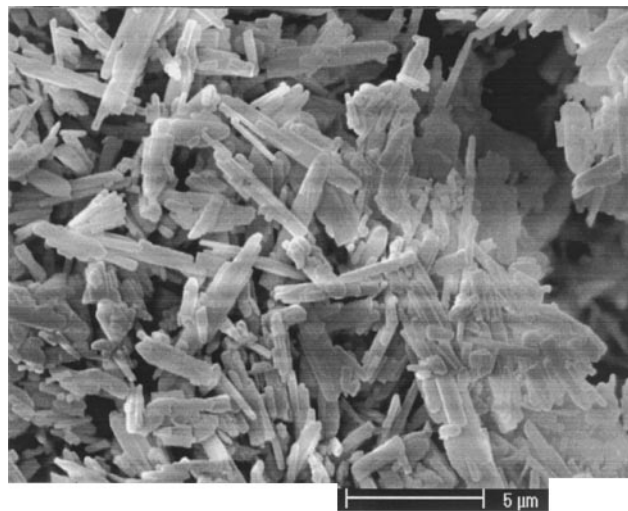


FIG. 5. SEM micrograph of the thorium hydroxide phosphate.

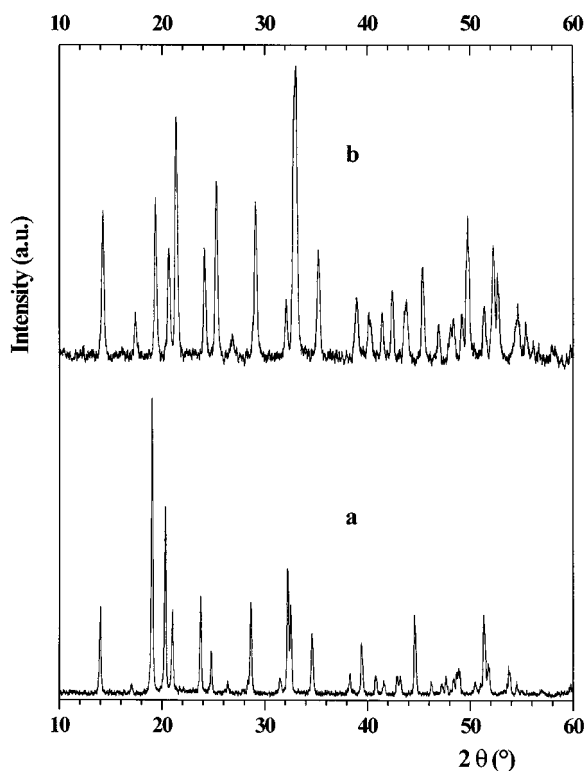


FIG. 6. XRD diagrams of the (a) thorium hydroxide phosphate and the (b) uranium hydroxide phosphate.

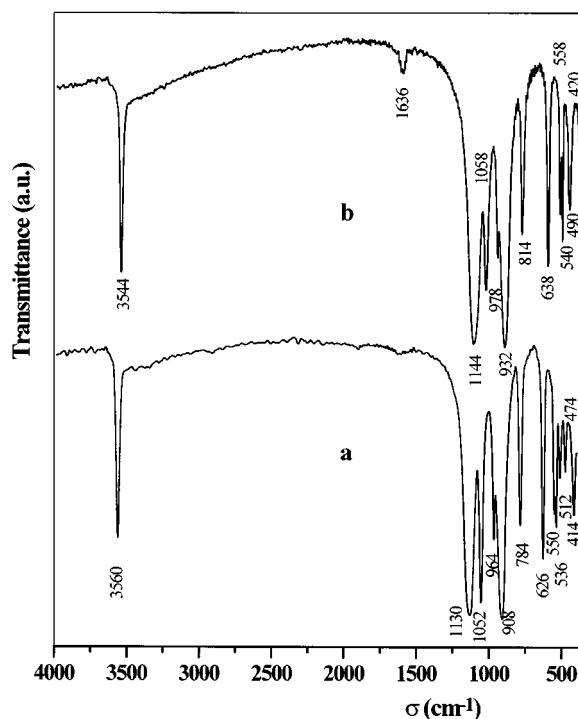


FIG. 7. IR spectra of the (a) thorium hydroxide phosphate and the (b) uranium hydroxide phosphate.

mode and to the (M)–O–H stretching modes as mentioned for many hydroxides and for magnesium hydroxide phosphate (15, 19). The vibration frequencies located at 784 and at 814 cm^{-1} are supposed to be the stretching modes of the Th–O and U–O bonds of the thorium and uranium hydroxide phosphates.

Besides these similarities, the frequencies at 1636 cm^{-1} assigned to the H–O–H bending mode appear only in the

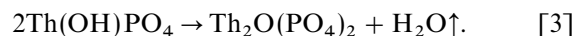
TABLE 4
Observed Frequencies and Band Assignment of the Thorium Hydroxide Phosphate (THOP) and the Uranium Hydroxide Phosphate (UHOP)

THOP	UHOP	Assignment
$\sigma(\text{cm}^{-1})$	$\sigma(\text{cm}^{-1})$	
3560	3544	stretching O–H and (Th)–O–H (U)–O–H
—	1636	bending H_2O
1130–908	1144–932	$\nu\text{P-O}$
784	814	stretching
626–414	638–420	Th–O; U–O $\delta\text{P-O}$

spectrum of the UHOP, which is a hydrated solid compound, whereas the THOP is an anhydrous compound.

Taking into account all the results presented, the proposed formula for the thorium phosphate synthesized in hydrothermal conditions is $\text{Th}(\text{OH})\text{PO}_4$.

The weight loss calculated from TGA curve (Fig. 8) of the THOP (average value $\Delta m = 2.6\%$) corresponds to only one mole of water per two moles of compound. On the DTA curve an endothermic band is simultaneously observed between 400 and 600°C. According to the loss of one mole of water, a decomposition reaction can be written



The XRD diagram (Fig. 9) recorded for the product heated at 650°C was compared to that of the diuranium oxide phosphate (DUOP), $\text{U}_2\text{O}(\text{PO}_4)_2$, (JCPDS File 47-0889). The unit-cell parameters of the DTOP were refined (13) considering the analogies observed between the XRD diagram of this compound and that of the DUOP, which was described in previously published works (24, 25, 28, 29). The indexation of the peaks observed, as well as the XRD data of the DTOP, are reported in Table 5. The unit cell of the DTOP can be defined as orthorhombic by comparison with the DUOP (symmetry group $Cmca$), with the following calculated parameters: $a = 7.177$ (4), $b = 9.225$ (5), and

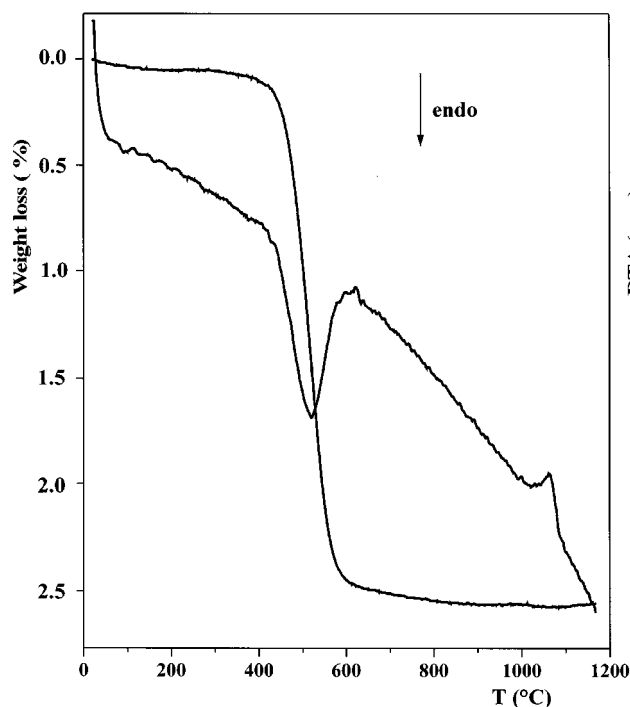


FIG. 8. TGA and DTA curves of the thorium hydroxide phosphate.

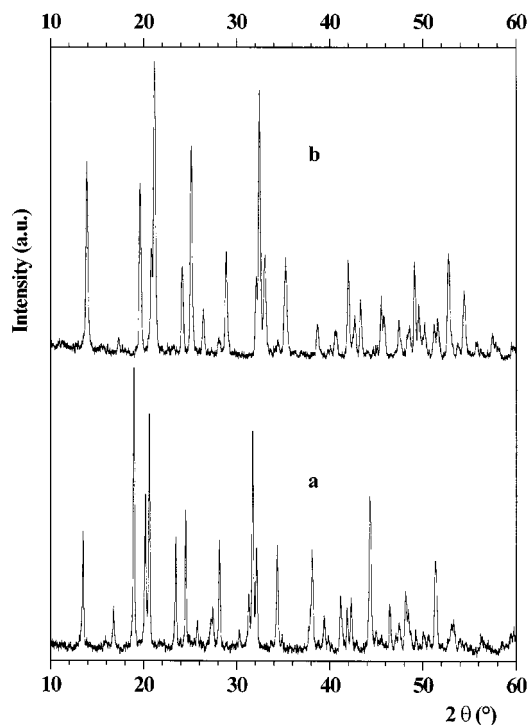


FIG. 9. XRD diagrams of the (a) dithorium oxide phosphate and the (b) diuranium oxide phosphate.

$c = 12.858(7) \text{ \AA}$. The unit cell volume is equal to $851(1) \text{ \AA}^3$, which corresponds to the cell volume increase of 4.6% compared to $\text{U}_2\text{O}(\text{PO}_4)_2$ (1.3% along a , 2.0% along b , and 1.3% along c). The calculated density was $5.23 \text{ g}\cdot\text{cm}^{-3}$ using the global formula $\text{Th}_2\text{P}_2\text{O}_9$ and $Z = 4$. The projection of the structure of $\text{M}_2\text{O}(\text{PO}_4)_2$ compounds along $[010]$ showed that this structure contains zig-zag chains of double edge-sharing MO_7 polyhedron related to PaCl_5 -type chains running along $[010]$. Within a chain, each tetravalent cation adopts the familiar seven-fold coordinated pentagonal bipyramidal arrangement (D_{5h}), of the nearest oxygen atom (28). For several cations, the existence of analogous compounds such as $\text{Zr}_2\text{O}(\text{PO}_4)_2$ (30, 31), $\text{Hf}_2\text{O}(\text{PO}_4)_2$ (32), $\text{U}_2\text{O}(\text{PO}_4)_2$ (28), and $\text{Np}_2\text{O}(\text{PO}_4)_2$ (6) have already been reported. In contrast, in the series of tetravalent actinide phosphates, it was impossible to synthesize, by the high-temperature method, an analogous plutonium compound because of the reduction of plutonium (IV) to the trivalent state, leading to the formation of PuPO_4 monazite structure (7).

From the study of $\text{M}_2\text{O}(\text{PO}_4)_2$ compounds ($M = \text{Zr}, \text{Hf}, \text{U}, \text{Np}$), it was possible to determine the variation of the unit cell volume as a function of the M^{4+} ionic radius in the seven-fold coordination. This variation is reported in Fig. 11. The corresponding equation obtained from the regression of the experimental data is

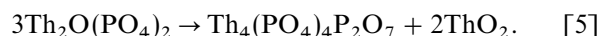
$$V(\text{\AA}^3) = 102(9) + 749(10) \times \text{VII} r_{M^{4+}}. \quad [4]$$

For Th^{4+} , in which the ionic radius in the seven-fold coordination is equal to 1.00 \AA (33), the unit cell volume calculated from Eq. [4] should be equal to $851(1) \text{ \AA}^3$. It is in very good agreement with the value obtained from the refinement of unit cell parameters.

Burdese and Borlera (34) synthesized a compound with the mole ratio $\text{P}/\text{Th} = 1/1$ at 1350°C , its formula was given as dithoryl diphosphate $(\text{ThO})_2\text{P}_2\text{O}_7$. The XRD diagrams of both solids $(\text{ThO})_2\text{P}_2\text{O}_7$ and DTOP are very different.

All the P–O vibration frequencies can be observed in the IR spectra of the DTOP and the DUOP. The Th–O or U–O stretching modes are shifted to 730 and 756 cm^{-1} , respectively (Table 6, Fig. 10).

On the DTA curve in Fig. 8, a broad exothermic peak occurs between 1000 and 1100°C , but no weight loss between 600 and 1200°C on the TGA curve is observed. TPD and ThO_2 rays appear in the XRD diagram (Fig. 12) of the DTOP heated at 1100°C . Thus, the exothermic peak was assigned to the decomposition of the DTOP into a two-phase system: TPD and thorium dioxide. The corresponding reaction can be written as



This is in good agreement with the thermal stability of the TPD up to 1250°C (11).

TABLE 5
X-Ray Powder Diffraction Data of the Dithorium
Oxide Phosphate (DTOP)

<i>h</i>	<i>k</i>	<i>l</i>	$2\theta_{\text{exp}}(^{\circ})$	$2\theta_{\text{calc}}(^{\circ})$	$d_{\text{exp}}(\text{\AA})$	I/I_0
0	0	2	13.78	13.77	6.42	44
1	1	1	17.05	17.10	5.20	19
0	2	0	19.24	19.24	4.61	100
0	2	1	20.46	20.45	4.34	62
1	1	2	20.89	20.90	4.25	79
0	2	2	23.74	23.74	3.74	39
2	0	0	24.81	24.81	3.59	43
1	1	3	26.08	26.07	3.41	6
0	0	4	27.73	27.75	3.21	15
0	2	3	28.43	28.43	3.14	41
2	0	2				
2	2	0	31.59	31.59	2.83	16
1	1	4	32.00	32.01	2.79	95
2	2	1	32.43	32.43	2.76	41
1	3	1				
2	2	2	34.65	34.67	2.59	42
1	3	2				
2	2	3	38.11	38.08	2.36	20
1	3	3	38.23	38.14	2.35	20
0	4	1	39.67	39.70	2.27	12
3	1	2	41.42	41.44	2.18	24
1	3	4	42.58	42.59	2.12	17
1	1	6	45.28	45.24	2.00	4
0	2	6	46.71	46.74	1.94	19
2	4	1	47.37	47.38	1.92	7
2	2	5	47.77	47.77	1.90	13
3	1	4	48.41	48.44	1.88	14
3	3	1	48.72	48.74	1.87	6
2	0	6	49.52	49.54	1.84	6
3	3	2	50.37	50.37	1.81	10
4	0	0	50.91	50.89	1.79	5
1	5	1	51.63	51.64	1.77	49
2	4	3				
1	5	2	53.35	53.36	1.72	14
0	4	5				
2	2	6	53.57	53.63	1.71	14
3	3	4	56.56	56.52	1.63	9

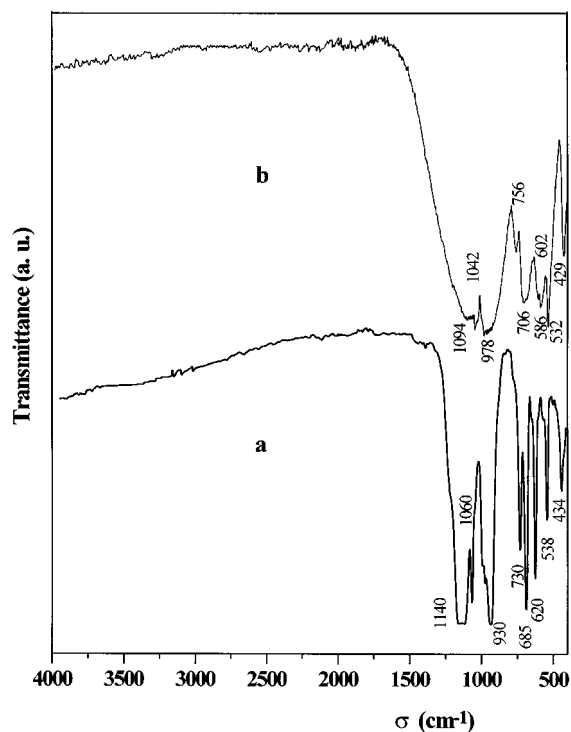


FIG. 10. IR spectra of the (a) dithorium oxide phosphate and the (b) diuranium oxide phosphate.

A quite similar decomposition was also observed for the diuranium oxide phosphate heated in argon at temperatures higher than 1350°C (24, 25, 29). Because a uranium phosphate analogous to TPD does not exist (7), under these conditions the decomposition process leads to the formation of UO_2 and a volatilization of P_4O_{10} .

CONCLUSIONS

Thorium phosphate–diphosphate (TPD) $\text{Th}_4(\text{PO}_4)_4\text{P}_2\text{O}_7$ is one of the matrices proposed for the radionuclide immobilization (1–4). It can be loaded with various cations (4), particularly tetravalent actinides (7). This compound is very resistant to water corrosion, which is very important

for long-term radioactive waste storage. Nevertheless, during the leaching tests in nitric acid, the TPD was transformed into an unknown crystallized compound. In this context it was necessary to identify and characterize the neoformed phase, which is supposed to be thorium phosphate–hydrogenphosphate (TPHP), $\text{Th}_2(\text{PO}_4)_2\text{HPO}_4$, or thorium hydroxide phosphate (THOP), $\text{Th}(\text{OH})\text{PO}_4$. In this objective, syntheses of these two compounds were performed in hydrothermal conditions in acidic solutions. These compounds were characterized by means of several techniques (EPMA, XRD, IR, TGA, DTA), by observing their behavior during heating treatment, as well as by

TABLE 6
Observed Frequencies of the Dithorium Oxide Phosphate
(DTOP) and the Diuranium Oxide Phosphate (DUOP)

DTOP	DUOP	Assignment
$\sigma(\text{cm}^{-1})$	$\sigma(\text{cm}^{-1})$	
1140–930	1094–978	$\nu\text{P-O}$
730	756	stretching
685–434	706–429	Th–O and U–O $\delta\text{P-O}$

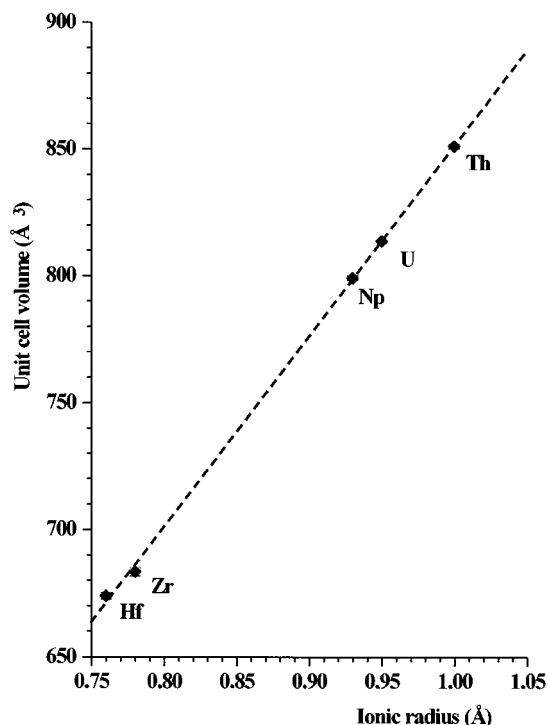


FIG. 11. Variation of the cell volume as function of the ionic radii ($r_{M^{+}}$) for various compounds $M_2O(PO_4)_2$.

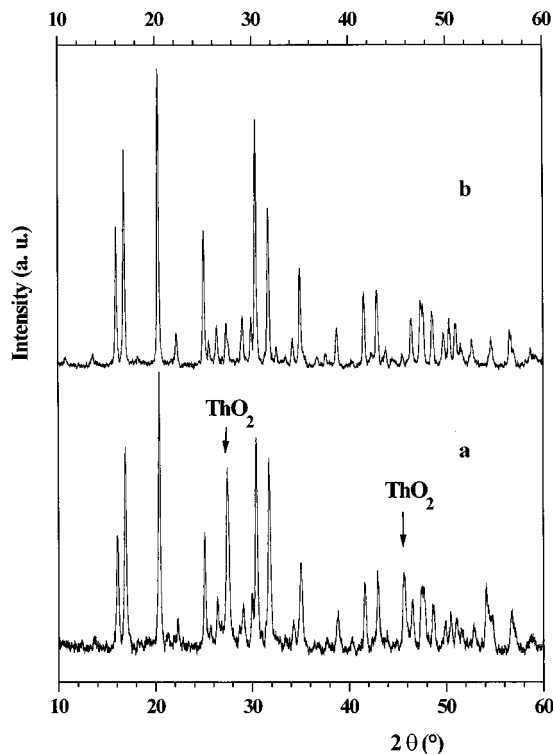


FIG. 12. XRD diagrams obtained after heating at 1100°C of (a) the dithorium oxide phosphate and of (b) the TPD.

comparison with analogous uranium phosphates. The results led to two crystallized pure phases: the thorium phosphate–hydrogenphosphate monohydrate $Th_2(PO_4)_2 \cdot H_2O$ and to the anhydrous THOP. The first phase was identical with the neoformed phase obtained during the dissolution of the TPD when the saturation of the solution is reached (8, 9). It controls the concentrations of thorium and phosphate ions in the solid-solution equilibrium. It seems that only the thorium phosphate–hydrogenphosphate is the less soluble compound in these experimental conditions. The calculated value of the solubility product $K_{s,0}^o$ of the TPHP is estimated to be $10^{-66.6 \pm 1.2}$ (8, 9, 27); its crystal structure is unknown. After heating at 950–1100°C, the TPHP is transformed into the thorium phosphate–diphosphate $Th_4(PO_4)_4P_2O_7$, as was already shown (11).

The formation of the thorium hydroxide phosphate was not observed during the leaching tests of the TPD. This compound is similar to the uranium hydroxide phosphate (UHOP). Its transformation at 650°C leads to the dithorium oxide phosphate $Th_2O(PO_4)_2$, which is probably isostructural with the diuranium oxide phosphate $U_2O(PO_4)_2$ (28).

REFERENCES

1. N. Dacheux, A. C. Thomas, B. Chassigneux, V. Brandel, and M. Genet, in "Environmental Issues and Waste Management Technologies IV" (J. C. Marra and G. T. Chandler, Eds.), Vol. 93, p. 373, American Chemical Society, Westerville, 1999.
2. N. Dacheux, A. C. Thomas, B. Chassigneux, E. Pichot, V. Brandel, and M. Genet, in "Scientific Basis for Nuclear Waste Management XXII" (D. J. Wronkiewicz and J. H. Lee, Eds.), Vol. 556, p. 85, Materials Research Society, Warrendale, 1999.
3. N. Dacheux, A. C. Thomas, B. Chassigneux, V. Brandel, and M. Genet, in "Environmental Issues and Waste Management Technologies V" (G. T. Chandler and X. Feng, Eds.), Vol. 107, p. 333, American Chemical Society, Westerville, 2000.
4. V. Brandel, N. Dacheux, M. Genet, E. Pichot, and A. C. Thomas, Global '99, in "International Conference on Future Nuclear Systems." Proceedings (CD-ROM), 1999.
5. P. Bénard, V. Brandel, N. Dacheux, S. Jaulmes, S. Launay, C. Lindecker, M. Genet, D. Louër, and M. Quarton, *Chem. Mater.* **8**, 181 (1996).
6. N. Dacheux, A. C. Thomas, V. Brandel, and M. Genet, *J. Nucl. Mater.* **257**, 108 (1998).
7. N. Dacheux, R. Podor, V. Brandel, and M. Genet, *J. Nucl. Mater.* **252**, 179 (1998).
8. A. C. Thomas, Ph.D. thesis, Université de Paris XI, France, IPNO-T-00.09, 2000.
9. A. C. Thomas, N. Dacheux, P. Le Coustumer, V. Brandel, and M. Genet, *J. Nucl. Mater.* **281**, 91 (2000).
10. B. Fourest, G. Lagarde, J. Peronne, V. Brandel, N. Dacheux, and M. Genet, *New J. Chem.* **23**, 645 (1999).
11. V. Brandel, N. Dacheux, M. Genet, E. Pichot, J. Emery, J. I. Buzaré, and R. Podor, *Chem. Mater.* **10**, 345 (1998).
12. V. Brandel, J. F. Le Dû, N. Dacheux, R. Podor, and M. Genet, *C. R. Acad. Sci. Paris* **1**, Série II c, 561–366 (1998).

13. M. Evain, "U-fit program," Institut des Matériaux de Nantes, France, 1992.
14. A. C. Chapman and L. E. Thirlwell, *Spectrochim. Acta* **20**, 937 (1964).
15. K. Nakamoto, "Infrared and Raman Spectra of Inorganic and Coordination Compounds," pp. 106, 115, 383, Wiley, New York, 1986.
16. D. E. Corbridge, "Topics in Phosphorus Chemistry" (E. Griffith and M. Grayson, Eds.), p. 275, Wiley Interscience, New York, 1966.
17. R. Hubin and P. Tarte, *Spectrochim. Acta* **23A**, 1815 (1967).
18. A. Rulmont, R. Cahay, M. Liegeois-Duyckaerts, and P. Tarte, *Eur. J. Solid State Inorg. Chem.* **28**, 207 (1991).
19. R. A. Nyquist and R. O. Kagel, "Infrared Spectra of Inorganic Compounds," pp. 163, 166, 230, 236, Academic Press, New York, 1971.
20. G. Alberti and U. Constantino, *J. Chromatogr.* **50**, 482 (1970).
21. A. K. De and K. Chowdhury, *J. Chromatogr.* **101**, 63 (1974).
22. F. Del Rey-Bueno, E. Villafranca-Sanchez, A. Mata-Arjona, E. Gonzalez-Pradas, and A. Garcia-Rodriguez, *Mater. Chem. Phys.* **21**, 49 (1989).
23. H. W. Dunn, X-ray diffraction data for some uranium compounds, ORNL (Oak Ridge National Laboratory, Oak Ridge, TN), Vol. 2092 (1956).
24. N. Dacheux, Ph.D. thesis, Université de Paris-Sud, France, IPNO-T-95.04, 1995.
25. N. Dacheux, V. Brandel, and M. Genet, *New J. Chem.* **19**, 15 (1995).
26. R. Podor, Ph.D. thesis, Université de Nancy I, France, 1994.
27. C. Thomas, N. Dacheux, V. Brandel, M. Genet, and J. Aupiais, to be published.
28. P. Bénard, D. Louër, N. Dacheux, V. Brandel, and M. Genet, *Anal. Quim.* **92**, 79 (1996).
29. V. Brandel, N. Dacheux, and M. Genet, *J. Solid State Chem.* **121**, 467 (1996).
30. W. Gerbert and E. Tillman, *Acta Crystallogr. Sect. B* **31**, 1768 (1975).
31. A. Ono and F. Nakamura, *Bull. Chem. Soc. Jpn.* **58**, 1051 (1985).
32. N. G. Chernorukov, I. A. Korshunov, and M. I. Zhuk, *Russ. J. Inorg. Chem.* **28**, 934 (1983).
33. R. D. Shannon, *Acta Crystallogr.* **5**, 12 (1975).
34. A. Burdese and M. L. Borlera, *Ann. Chim. Roma* **53**, 344 (1963).